

tubules, which is essential for establishing cell polarity. The role of Apc is unclear; it could directly affect microtubule dynamics^{25,26}, or—perhaps through EB1—interact with the dynactin–dynein complex, which is required for centrosome reorientation^{5,27,28}. These observations link together two important signalling pathways that have been independently implicated in controlling cell polarity during the development of multicellular organisms: Cdc42–Par proteins on one hand², and GSK-3– β -catenin–Apc on the other¹⁰. The essential role described here for Apc in regulating the polarity of migrating cells may be an important aspect of its functional contribution to human cancer. □

Methods

Materials

We used the following reagents: anti- α -tubulin (Sigma), anti-GSK-3 β , anti- β -catenin, anti-EB1 (all Transduction Labs), anti-PKC ζ , anti-Cdc42 (both Santa Cruz Biotechnology), anti-pericentrin (BabCO), anti-phospho-GSK-3 β (Ser 9) (Biosource), anti-Apc (I. Näthke) and anti-Par6C (amino acids 2–16; P. Aspenström), GF109203X, RO 31-8220 and SB216763 (all Calbiochem), PKC ζ pseudo-substrate (Biosource), toxins B10463 and B1470 (C. von Eichel-Streiber), GSK-3 constructs (V. M. Lee and R. Kypta) and Apc constructs (B. M. Gumbiner). GTPases, Par6 and PKC ζ constructs have been described previously⁵.

Cell culture and scratch-induced migration

Primary astrocyte monolayers and scratch assays have been described previously⁵. Individual wounds around 300 μ m wide were made with a microinjection needle, and wound closure occurred 16–24 h later. For biochemical analysis, multiple wounds were made with an eight-channel pipette (with 2- μ l tips) scratched several times across a 90-mm dish. Centrosomes were localized using anti-pericentrin antibody⁵, and those within the quadrant facing the wound were scored as positive. We examined 300 cells for each condition. To assess polarized morphology, astrocytes were microinjected with pEGFP as a control or with the indicated DNA constructs and biotin-dextran, and were fixed 8 h later. Cells expressing these constructs were scored as protruding when their length was at least four times their width.

Immunoprecipitation

Cells were washed with ice-cold PBS containing 1 mM orthovanadate and lysed at 4 °C in buffer (10 mM Tris-HCl, pH 7.5, 140 mM NaCl, 1 mM orthovanadate, 1% Nonidet-P40, 2 mM phenylmethylsulphonyl fluoride, 5 mM EDTA, 20 μ g ml⁻¹ aprotinin, 20 μ g ml⁻¹ leupeptin). Nuclei were discarded after centrifugation at 10,000g for 10 min. Lysates were incubated for 2 h at 4 °C with specific antibodies and protein G Sepharose, and immunoprecipitates were collected by centrifugation and were analysed on 8% SDS–polyacrylamide gel electrophoresis gels.

Received 25 November 2002; accepted 14 January 2003; doi:10.1038/nature01423.

Published online 29 January 2003.

- Etienne-Manneville, S. & Hall, S. Rho GTPases in cell biology. *Nature* **420**, 629–635 (2002).
- Ohno, S. Intercellular junctions and cellular polarity: the PAR–aPKC complex, a conserved core cassette playing fundamental roles in cell polarity. *Curr. Opin. Cell Biol.* **13**, 641–648 (2001).
- Gotta, M., Abraham, M. C. & Ahninger, J. CDC-42 controls early cell polarity and spindle orientation in *C. elegans*. *Curr. Biol.* **11**, 482–488 (2001).
- Kay, A. J. & Hunter, C. P. CDC-42 regulates PAR protein localization and function to control cellular and embryonic polarity in *C. elegans*. *Curr. Biol.* **11**, 474–481 (2001).
- Etienne-Manneville, S. & Hall, A. Integrin-mediated Cdc42 activation controls cell polarity in migrating astrocytes through PKC ζ . *Cell* **106**, 489–498 (2001).
- Dominguez, I., Itoh, K. & Sokol, S. Y. Role of glycogen synthase kinase 3 β as a negative regulator of dorsoventral axis formation in *Xenopus* embryos. *Proc. Natl Acad. Sci. USA* **92**, 8498–8502 (1995).
- Emily-Fenouil, F., Ghigliione, C., Lhomond, G., Lepage, T. & Gache, C. GSK3 β /shaggy mediates patterning along the animal-vegetal axis of the sea urchin embryo. *Development* **125**, 2489–2498 (1998).
- He, X., Saint-Jeannet, J.-P., Woodgett, J. R., Varmus, H. E. & Dawid, I. Glycogen synthase kinase-3 and dorsoventral patterning in *Xenopus* embryos. *Nature* **374**, 617–622 (1995).
- Pierce, S. B. & Kimelman, D. Regulation of Spemann organizer formation by intracellular Xgsk-3. *Development* **121**, 755–765 (1995).
- Ferkey, D. M. & Kimelman, D. GSK-3: new thoughts on an old enzyme. *Dev. Biol.* **225**, 471–479 (2000).
- Oriente, F. et al. Insulin receptor substrate-2 phosphorylation is necessary for protein kinase C ζ activation by insulin in L6hIR cells. *J. Biol. Chem.* **276**, 37109–37119 (2001).
- Harwood, J. A. Regulation of GSK-3: a cellular multiprocessor. *Cell* **105**, 821–824 (2001).
- Troussard, A. A., Tan, C., Yoganathan, T. N. & Dedhar, S. Cell–extracellular matrix interactions stimulate the AP-1 transcription factor in an integrin-linked kinase- and glycogen synthase kinase 3-dependent manner. *Mol. Cell Biol.* **19**, 7420–7427 (1999).
- Li, L. et al. Axin and Frat1 interact with Dvl and GSK, bridging Dvl to GSK in the Wnt-mediated regulation of LEF-1. *EMBO J.* **18**, 4233–4240 (1999).
- Moon, R. T., Bowerman, B., Boutros, M. & Perrimon, N. The promise and perils of Wnt signaling through β -catenin. *Science* **296**, 1644–1646 (2002).
- Polakis, P. Wnt signaling and cancer. *Genes Dev.* **14**, 1837–1851 (2000).
- Munemitsu, S., Albert, I., Souza, B., Rubinfeld, B. & Polakis, P. Regulation of intracellular β -catenin levels by the adenomatous polyposis coli (APC) tumour-suppressor protein. *Proc. Natl Acad. Sci. USA* **92**, 3046–3050 (1995).
- Rubinfeld, B. et al. Binding of GSK3 β to the APC- β -catenin complex and regulation of complex assembly. *Science* **272**, 1023–1026 (1996).

- Bienz, M. The subcellular destinations of APC proteins. *Nature Rev. Mol. Cell Biol.* **3**, 328–338 (2002).
- Mogensen, M. M., Tucker, J. B., Mackie, J. B., Prescott, A. R. & Nathke, I. S. The adenomatous polyposis coli protein unambiguously localizes to microtubule plus ends and is involved in establishing parallel arrays of microtubule bundles in highly polarized epithelial cells. *J. Cell Biol.* **157**, 1041–1048 (2002).
- Su, L. K. et al. APC binds to the novel protein EB1. *Cancer Res.* **55**, 2972–2977 (1995).
- Barth, A. I. M., Siemers, K. A. & Nelson, W. J. Dissecting interactions between EB1, microtubules and APC in cortical clusters at the plasma membrane. *J. Cell Sci.* **115**, 1583–1590 (2002).
- Wagner, U., Utton, M., Gallo, J.-M. & Miller, C. C. J. Cellular phosphorylation of Tau by GSK-3 β influences tau binding to microtubules and microtubule organisation. *J. Cell Sci.* **109**, 1537–1543 (1996).
- Lucas, F. R., Goold, R. G., Gordon-Weeks, P. R. & Salinas, P. C. Inhibition of GSK-3 β leading to the loss of phosphorylated MAP-1B is an early event in axonal remodelling induced by WNT-7a or lithium. *J. Cell Sci.* **111**, 1351–1361 (1998).
- Nakamura, M., Zhou, X. Z. & Lu, K. P. Critical role for the EB1 and APC interaction in the regulation of microtubule polymerization. *Curr. Biol.* **11**, 1062–1067 (2001).
- Zumbrunn, J., Kinoshita, K., Hyman, A. A. & Nathke, I. S. Binding of the adenomatous polyposis coli protein to microtubules increases microtubule stability and is regulated by GSK3 β phosphorylation. *Curr. Biol.* **11**, 44–49 (2001).
- Palazzo, A. F. et al. Cdc42, dynein, and dynactin regulate MTOC reorientation independent of Rho-regulated microtubule stabilization. *Curr. Biol.* **11**, 1536–1541 (2001).
- Berrueta, L., Tirnauer, J. S., Schuyler, S. C., Pellman, D. & Bierer, B. E. The APC-associated protein EB1 associates with components of the dynactin complex and cytoplasmic dynein intermediate chain. *Curr. Biol.* **9**, 425–428 (1999).

Acknowledgements This work was supported by a Cancer Research UK programme grant, the Medical Research Council and by an EMBO Long-Term Fellowship (S.E.-M.). We thank S. Martin, V. M. Lee, R. Kypta, B. M. Gumbiner, P. Aspenström, I. Näthke and C. von Eichel-Streiber for plasmids and reagents.

Competing interests statement The authors declare that they have no competing financial interests.

Correspondence and requests for materials should be addressed to A.H. (e-mail: alan.hall@ucl.ac.uk).

Structure of the extracellular region of HER2 alone and in complex with the Herceptin Fab

Hyun-Soo Cho^{*†}, Karen Mason[‡], Kasra X. Ramyar^{*}, Ann Marie Stanley^{*}, Sandra B. Gabelli^{*}, Dan W. Denney Jr[‡] & Daniel J. Leahy^{*†}

^{*} Department of Biophysics and Biophysical Chemistry, and [†] Howard Hughes Medical Institute, The Johns Hopkins University School of Medicine, 725 North Wolfe Street, Baltimore, Maryland 21205, USA

[‡] Genitope Corporation, 525 Penobscot Drive, Redwood City, California 94063, USA

HER2 (also known as Neu, ErbB2) is a member of the epidermal growth factor receptor (EGFR; also known as ErbB) family of receptor tyrosine kinases, which in humans includes HER1 (EGFR, ERBB1), HER2, HER3 (ERBB3) and HER4 (ERBB4)¹. ErbB receptors are essential mediators of cell proliferation and differentiation in the developing embryo and in adult tissues², and their inappropriate activation is associated with the development and severity of many cancers³. Overexpression of HER2 is found in 20–30% of human breast cancers, and correlates with more aggressive tumours and a poorer prognosis⁴. Anticancer therapies targeting ErbB receptors have shown promise, and a monoclonal antibody against HER2, Herceptin (also known as trastuzumab), is currently in use as a treatment for breast cancer⁵. Here we report crystal structures of the entire extracellular regions of rat HER2 at 2.4 Å and human HER2 complexed with the Herceptin antigen-binding fragment (Fab) at 2.5 Å. These structures reveal a fixed conformation for HER2 that resembles a ligand-activated state, and show HER2 poised to interact with other ErbB receptors in the absence of direct ligand

binding. Herceptin binds to the juxtamembrane region of HER2, identifying this site as a target for anticancer therapies.

ErbB receptors comprise an extracellular region of about 630 amino acids that contains four domains (I/L1, II/CR1, III/L2 and IV/CR2) arranged as a tandem repeat of a two-domain unit, a single membrane-spanning region and a cytoplasmic tyrosine kinase⁶. Binding of ligand to the extracellular region induces receptor dimerization and activation of the cytoplasmic kinase, which in turn leads to autophosphorylation and initiation of downstream signalling events^{1,7}. Over 11 different EGF-like ErbB ligands have been identified⁸. Many of these ligands activate homodimeric receptor complexes, but most, if not all, also signal through heteromeric receptor complexes that include HER2. Despite functioning as a universal ErbB co-receptor, HER2 is the only ErbB receptor for which a high-affinity ligand has not been found. HER2 is also unusual among ErbB receptors in its ability to transform cells in a ligand-independent manner when overexpressed^{3,9}.

Recent crystal structures of extracellular regions of HER1 (sHER1) complexed with either EGF¹⁰ or transforming growth factor- α (TGF- α)¹¹ reveal ligand bound to domains I and III, and a long, finger-like projection from domain II mediating an inter-receptor dimer. By contrast, crystal structures of non-activated forms of sHER1 (ref. 12) and sHER3 (ref. 13) reveal this finger-like projection from domain II making an intramolecular contact with a pocket on domain IV. Together these observations suggest a model for receptor activation in which unliganded receptors exist in an autoinhibited or 'closed' form that undergoes substantial domain rearrangement to an 'open' form on ligand binding. This rearrangement brings domains I and III close together, breaking the domain II–IV interaction and freeing the domain II projection to participate in receptor dimerization and initiation of signal transduction.

To provide a molecular basis for understanding the role of HER2 in signalling and cancer, we have determined the crystal structure of rat sHER2 at 2.4 Å resolution and human sHER2 complexed with the Fab fragment of the anticancer monoclonal antibody Herceptin at 2.5 Å resolution. Both rat and human sHER2 were expressed in mammalian cells and enzymatically deglycosylated before crystallization. The crystal structures were solved by molecular replacement using the A5B7 Fab structure¹⁴ and the individual domains of sHER3 (ref. 13) as search models. The $R_{\text{cryst}}/R_{\text{free}}$ values for rat sHER2 and the human sHER2–Herceptin complex are 0.226/0.282 and 0.223/0.286, respectively. Complete data collection and refinement statistics are available as Supplementary Information.

The structures of rat and human sHER2 (Fig. 1) superimpose

well. A total of 448 residues between amino acids 1 and 542 superimpose with a root mean square deviation (r.m.s.d.) of C α positions of 0.99 Å, with the principal variation being an approximately 7° change in the angle between domains III and IV. The appearance of such similar structures in different crystal environments indicates that the interdomain relationships in sHER2 are relatively fixed.

Comparison of the sHER2 structures with the sHER3 (ref. 13) and sHER1 (ref. 12) structures indicates that domains I and II adopt a relatively fixed interdomain relationship, as do domains III and IV, but that the relative orientation of these domain pairs varies widely (Fig. 2). Some spine-like bending of the cysteine-rich domains is also observed. The relative orientations of domain II to I and domain IV to III appear stabilized in part by conserved tryptophan residues that extend from domain II (Trp 183) and domain IV (Trp 499) to contact conserved tryptophan residues in the hydrophobic cores of domain I (Trp 147) and domain III (Trp 460), respectively. Conformational change in ErbB receptors thus seems to involve rigid-body movements of the domain I–II pair relative to the domain III–IV pair about a pivot between domains II and III. The differences in main-chain conformation that account for this pivot occur within residues 316–323 of sHER2 (307–314 of sHER3), with the largest rotation occurring about Val 320 (Ala 311 in sHER3).

The domain II–IV contact that restricts the domain arrangement in non-activated sHER1 and sHER3 is absent in sHER2 (Figs 1 and 2c), and the orientation of domains I/II relative to domains III/IV in sHER2 appears to be determined chiefly by a large interface between domains I and III. Failure to conserve two key residues in the domain IV contact region (Gly 563 and His 565 of HER3 are replaced with Pro and Phe, respectively, in HER2) may explain the absence of the domain II–IV contact in HER2 (ref. 13). Several features of the HER2 domain I–III interface, which is made up of a core of hydrophobic residues surrounded by hydrophilic contacts, suggest that it is stable; in addition to being preserved in two different crystal lattices, it buries 1,167 Å² of surface area and gives a very high shape complementarity parameter (0.75; ref. 15). Orthogonal views of this interface and an alignment of the sequences composing it are available as Supplementary Information.

The proximity and relative orientation of domains I and III in sHER2 are very similar to the domain arrangement observed in the structures of sHER1 complexed with either TGF- α ¹¹ or EGF¹⁰ (Fig. 3). Recent biochemical evidence implicates domain IV in mediating inter-receptor dimers¹⁶, but domain IV is either not present¹¹ or not visible¹⁰ in the ligand-activated structures of

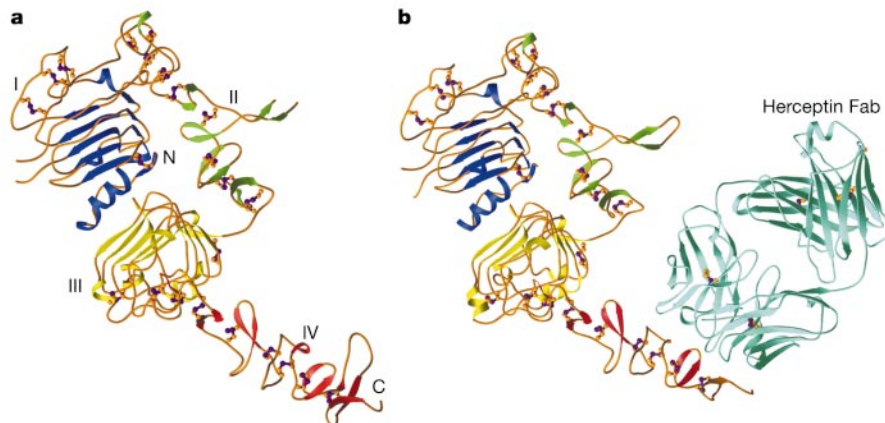


Figure 1 The structure of rat and human sHER2. **a**, Ribbon diagram of rat sHER2. Domains I (blue), II (green), III (yellow) and IV (red), and the amino and carboxy termini, are indicated. Disulphide bonds are shown in purple and gold. **b**, Ribbon diagram of the

human sHER2 (coloured as in **a**) and Herceptin Fab (cyan) complex. Figures 1 and 2c were made using the program Ribbons²⁹.

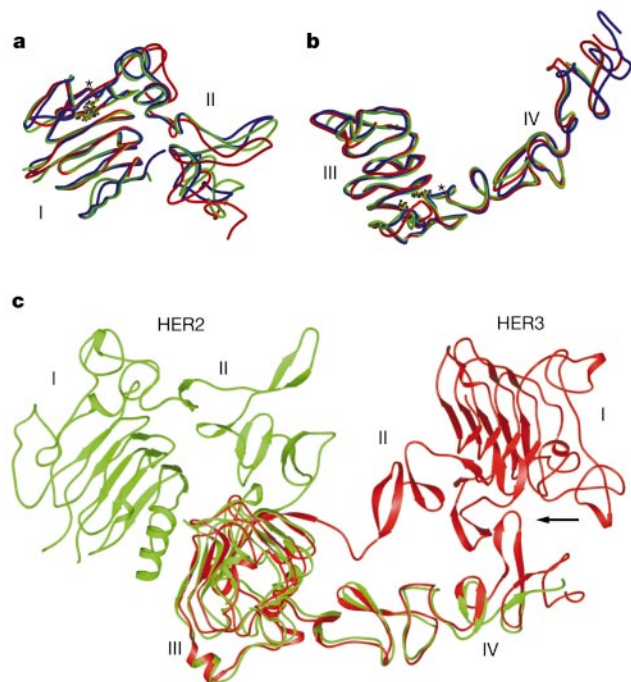


Figure 2 Superposition of different ErbB receptors. **a**, Superposition of domains I and II of sHER1 (ref. 12; blue), sHER2 (green) and sHER3 (ref. 13; red). Ball-and-stick models of conserved tryptophan residues from each receptor are also shown and are indicated by an asterisk. **b**, Superposition of domains III and IV of sHER1, sHER2 and sHER3 coloured as in **a**. **c**, Human sHER2 (green) and sHER3 (red) after superposition of domains III and IV. Individual domains are numbered and the 'snap-like' contact between domains II and IV of sHER3 is indicated by an arrow. Figures 2a, b and 3 are made with the program MOLSCRIPT³⁰.

sHER1. Conservation of the relative orientation of domains III and IV in ErbB receptors (Fig. 2b) allows positioning of domain IV in the ligand-induced EGFR dimer by superposing domain III of the sHER2 domain III–IV pair with domain III of the EGFR dimer. This superposition indicates that the carboxy termini of domain IV are brought into close proximity in this dimer (see Supplementary Information), which is consistent with a model in which signalling is initiated by juxtaposition of the receptor transmembrane regions, presumably in a favoured orientation.

The exposed domain II loop that mediates inter-receptor dimers of sHER1 is also exposed in sHER2 but does not mediate a similar HER2 dimer in either crystal form, indicating a dimerization constant greater than about 10 mM. The EGFR dimer is mediated entirely by residues from domain II (refs 10, 11), and the only residue at the dimer interface not conserved between EGFR and HER2 is Arg 285 of EGFR, which is Leu in HER2. Mutation of Arg 285 to Ser reduces ligand-induced phosphorylation of EGFR¹⁰, suggesting that Leu at this position in HER2 is likely to be at least partly responsible for the absence of sHER2 homodimers. Given the symmetry of the inter-receptor dimer, mutations affecting dimerization would be doubly harmful to homodimers relative to heterodimers, which may explain the apparent ability of HER2 to participate in heterodimeric complexes. It is also possible that HER2 interacts with other ErbB receptors either indirectly or through different contact regions, but the highly conserved contact residues in the domain II loop make these alternatives seem less probable.

The constitutive open structure of HER2 helps to explain several of its singular properties. The absence of a high-affinity ligand for HER2 can be explained by its fixed open structure, which does not require ligand binding to release an autoinhibited conformation. By adopting a fixed conformation, HER2 must be intrinsically capable

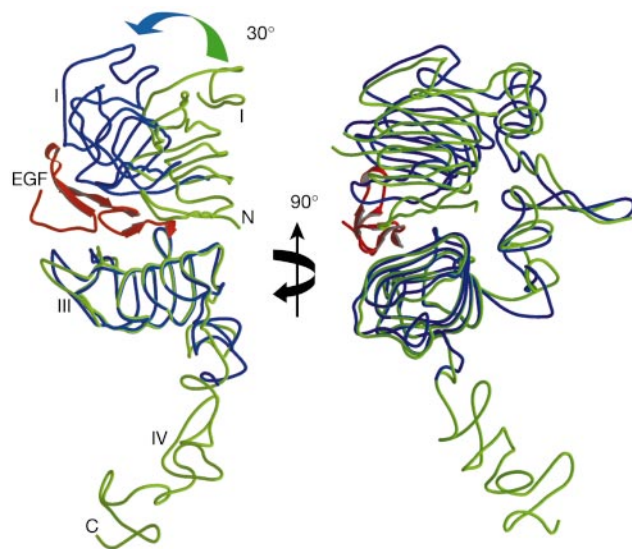


Figure 3 Relationship of sHER2 to ligand-activated sHER1. Orthogonal views of sHER2 (green) and sHER1 (blue) with EGF (red) bound¹⁰ after superposition of domain III. Domain II has been omitted from the figure on the left for clarity.

of interacting with any binding partners that become available, explaining its readiness to serve as a co-receptor with each of the other ErbB receptors in the absence of direct ligand binding. Overexpression of HER2 in tissue culture cells leads to HER2 activation and a transformed phenotype, but overexpression of HER1 or HER3 is not transforming unless ligand is added^{3,9}. Maintenance of HER1 and HER3 in the closed conformation in the absence of ligand is clearly a barrier to autoactivation. Absence of this autoinhibited conformation for HER2 eliminates this barrier, which accounts in part for its transforming potential when overexpressed.

The anti-HER2 monoclonal antibody Herceptin has an antiproliferative effect on cells transformed by overexpression of HER2, and is an effective treatment for human breast cancer⁵. The mechanism of Herceptin action is thought to involve many processes, including antibody-mediated cytotoxicity and blocking receptor aggregation, but stimulation of HER2 endocytosis and removal of HER2 from the cell surface seems to be a principal element of its effectiveness^{17,18}. Monovalent Herceptin Fab fragments do not possess the antiproliferative properties of the whole Herceptin antibody, suggesting that either receptor crosslinking is an important feature of Herceptin activity or that divalence is needed to increase its apparent affinity. Herceptin also inhibits activation of HER2 through cleavage of the juxtamembrane region of the extracellular domain, a process that normally occurs at a low level but increases when HER2 is overexpressed¹⁹.

Herceptin binds HER2 on the C-terminal portion of domain IV at a site that encompasses the binding pocket for the extended domain II loop in inactive states of HER3 and HER1 (Figs 1b and 4). This interaction buries 1,350 Å² of surface area over a long groove and possesses an unusually high shape complementarity (0.76; ref. 15) for antigen–antibody interactions. The interaction is mediated by three regions of HER2; loops formed by residues 557–561 and 570–573, and the base of a loop formed by residues 593–603. Interactions formed by the first and third loop are primarily electrostatic, whereas the second loop makes mostly hydrophobic contacts in a pocket formed by the CDR3 loops of heavy and light chains of the antibody. Binding of Herceptin to the juxtamembrane region may sufficiently crosslink the HER2 receptor to facilitate engagement of the endocytotic machinery while avoiding undue kinase activation by providing a steric barrier

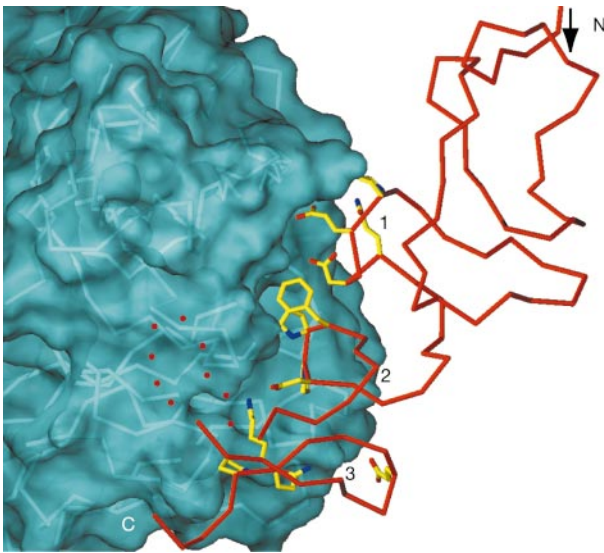


Figure 4 The Herceptin-binding site. The backbone of sHER2 is shown in red with side chains of residues contacting the Herceptin Fab added. The surface of the Herceptin Fab fragment is shown in cyan. The N and C termini of the displayed region of HER2 are indicated, as are the three loop regions of HER2 (residues 557–561 (loop 1), 570–573 (loop 2) and 593–603 (loop 3)) that contact the Herceptin Fab fragment. An eight-residue loop not visible in the structure is indicated by red dots. This figure was made with the program SPOCK.

to direct interaction of the transmembrane regions, which may be required for optimal signalling²⁰. Binding at this site will also sterically block activation of HER2 by proteolytic cleavage of its extracellular region, and may disrupt interactions between HER2 and other proteins.

The structures of sHER2 and the Herceptin Fab fragment provide a basis for the design of new therapeutics to target HER2. Antibodies raised specifically against the juxtamembrane region of ErbB receptors may prove more likely to modulate ErbB receptor behaviour, and knowledge of the precise HER2–Herceptin contacts may allow design or selection of Herceptin variants with higher affinity and improved therapeutic properties. The Herceptin-binding site encompasses a pocket-like structure homologous to the domain II loop-binding pocket of other ErbB receptors, which may accommodate binding of small, perhaps peptide-based molecules with reasonable affinity. Multivalent forms of such a compound may provide a new weapon against HER2-overexpressing cancers. Furthermore, if the exposed domain II loop of HER2 proves important for mediating interactions of HER2 with itself or with other ErbB receptors, agents targeting this loop, for example small peptides or peptide analogues derived from this region, may inhibit such interactions. □

Methods

Expression of rat sHER2

Residues –22–635 of rat HER2 followed by a 7-His tag were expressed in BW5147.G.1.4 cells using HI-GET technology²¹. sHER2 was purified using Ni-NTA resin, chromatographed on a gel-filtration column, deglycosylated with PNGase F, re-chromatographed on a gel-filtration column, concentrated to 5 mg ml⁻¹, and dialysed against 10 mM Tris, pH 7.5. Crystals of sHER2 were grown by the hanging-drop vapour diffusion method using drops with equal parts protein solution and 15–30% PEG 4000, 50 mM sodium citrate, pH 5.4, and 10 mM EDTA. Crystals grew in space group *P*₂₁₂₁ with cell dimensions *a* = 130.87, *b* = 116.40, *c* = 55.37 Å.

Expression of human sHER2

Residues 1–631 of human HER2 were expressed as a fusion protein with human growth hormone in Lec1 cells using the pSGH0 expression vector²². Human sHER2 fusion protein was purified using Ni-NTA resin, cleaved by TEV protease, and re-chromatographed on a gel filtration column. Purified sHER2 was dialysed into 10 mM sodium citrate, pH 5.5 and 50 mM NaCl, treated with endoglycosidase H,

re-chromatographed on a gel filtration column, concentrated to 3.8 mg ml⁻¹, and dialysed against 10 mM Tris, pH 7.5, and 50 mM NaCl.

The sHER2–Herceptin Fab complex

Herceptin (also known as trastuzumab) was purchased from Genentech. Ten milligrams of Herceptin were cleaved with papain, and the Fab fragment was purified by anion exchange chromatography using a Resource-Q column. Human sHER2 was mixed with an excess of the Herceptin Fab, and the complex was purified by gel-filtration chromatography. This complex was dialysed against 10 mM Tris, pH 7.5, and concentrated to 4 mg ml⁻¹. Crystals were grown by the hanging-drop vapour diffusion method using equal parts protein solution and 20–30% PEG 5000 MME, 0.1 M MES, pH 6.5, and 0.2 M ammonium sulphate. Crystals grew in space group *P*₂₁₂₁ with cell dimensions *a* = 66.17, *b* = 109.77, *c* = 175.14 Å.

Structure determination and refinement

Diffraction data were collected at beamlines X4A and X25 at the National Synchrotron Light Source (NSLS) at Brookhaven National Laboratory. The structures of rat sHER2 and human sHER2 complexed with the Herceptin Fab fragment were determined by molecular replacement using AMORE²³, CNS²⁴ and MOLREP²⁵ with individual domains of sHER3¹² and the A5B7 Fab¹³ as search models. Alternate sessions of model building using O²⁶ and refinement using CNS resulted in placement of nearly all of the sHER2 and Herceptin amino acids. Final rounds of refinement were carried out using TLS refinement as implemented in REFMAC5²⁷ with anisotropic motion tensors refined for each of the four sHER2 domains.

The final rat sHER2 structure consists of residues 1–101, 113–253 and 259–608, 85 water molecules, and 3 *N*-acetylglucosamine moieties. The final human HER2–Herceptin Fab structure consists of residues 1–101, 111–302, 306–360, 365–580 and 591–607 of sHER2, antibody residues 1–211 and 1–223 for the light and heavy chains, respectively, 79 water molecules, one sulphate ion, and two *N*-acetylglucosamine moieties. All stereochemical parameters analysed by the program PROCHECK²⁸ are within or exceed normal ranges, and the percentage of residues in the most favoured regions of the Ramachandran plot are 86.8% and 84.8% for rat sHER2 and human sHER2 plus the Herceptin Fab, respectively.

Received 17 September; accepted 17 December 2002; doi:10.1038/nature01392.

- Yarden, Y. & Sliwkowski, M. X. Untangling the ErbB signalling network. *Nature Rev. Mol. Cell Biol.* **2**, 127–137 (2001).
- Olayioye, M. A., Neve, R. M., Lane, H. A. & Hynes, N. E. The ErbB signaling network: receptor heterodimerization in development and cancer. *EMBO J.* **19**, 3159–3167 (2000).
- Tang, C. K. & Lippman, M. E. in *Hormones and Signaling* (ed. O'Malley, B. W.) 113–165 (Academic, San Diego, 1998).
- Slamon, D. J. *et al.* Human breast cancer: correlation of relapse and survival with amplification of the HER-2/neu oncogene. *Science* **235**, 177–182 (1987).
- Slamon, D. J. *et al.* Use of chemotherapy plus a monoclonal antibody against HER2 for metastatic breast cancer that overexpresses HER2. *N. Engl. J. Med.* **344**, 783–792 (2001).
- Carpenter, G. Receptors for epidermal growth factor and other polypeptide mitogens. *Annu. Rev. Biochem.* **56**, 881–914 (1987).
- Schlessinger, J. Cell signaling by receptor tyrosine kinases. *Cell* **103**, 211–225 (2000).
- Jones, J. T., Akita, R. W. & Sliwkowski, M. X. Binding specificities and affinities of egf domains for ErbB receptors. *FEBS Lett.* **447**, 227–231 (1999).
- Di Fiore, P. P. *et al.* erbB-2 is a potent oncogene when overexpressed in NIH/3T3 cells. *Science* **237**, 178–182 (1987).
- Ogiso, H. *et al.* Crystal structure of the complex of human epidermal growth factor and receptor extracellular domains. *Cell* **110**, 775–787 (2002).
- Garrett, T. P. *et al.* Crystal structure of a truncated epidermal growth factor receptor extracellular domain bound to transforming growth factor α . *Cell* **110**, 763–773 (2002).
- Ferguson, K. M. *et al.* EGF activates its receptor by relieving auto-inhibition of ectodomain dimerization. *Mol. Cell* (in the press).
- Cho, H. S. & Leahy, D. J. Structure of the extracellular region of HER3 reveals an interdomain tether. *Science* **297**, 1330–1333 (2002).
- Banfield, M. J., King, D. J., Mountain, A. & Brady, R. L. VL:VH domain rotations in engineered antibodies: crystal structures of the Fab fragments from two murine antitumor antibodies and their engineered human constructs. *Proteins* **29**, 161–171 (1997).
- Lawrence, M. C. & Colman, P. M. Shape complementarity at protein/protein interfaces. *J. Mol. Biol.* **234**, 946–950 (1993).
- Berezov, A. *et al.* Disabling receptor ensembles with rationally designed interface peptidomimetics. *J. Biol. Chem.* **277**, 28330–28339 (2002).
- Harari, D. & Yarden, Y. Molecular mechanisms underlying ErbB2/HER2 action in breast cancer. *Oncogene* **19**, 6102–6114 (2000).
- Sliwkowski, M. X. *et al.* Nonclinical studies addressing the mechanism of action of Trastuzumab (Herceptin). *Semin. Oncol.* **26**, 60–70 (1999).
- Molina, M. A. *et al.* Trastuzumab (Herceptin), a humanized anti-Her2 receptor monoclonal antibody, inhibits basal and activated Her2 ectodomain cleavage in breast cancer cells. *Cancer Res.* **61**, 4744–4749 (2001).
- Burke, C. L., Lemmon, M. A., Coren, B. A., Engelman, D. M. & Stern, D. F. Dimerization of the p185neu transmembrane domain is necessary but not sufficient for transformation. *Oncogene* **14**, 687–696 (1997).
- Denney, D. W. Jr Gene amplification methods. US patent 5,776,746 (1998).
- Leahy, D. J., Dann, C. E., Longo, P., Perman, B. & Ramyar, K. X. A mammalian expression vector for expression and purification of secreted proteins for structural studies. *Protein Expr. Purif.* **20**, 500–506 (2000).
- Navaza, J. AMoRe: an automated package for molecular replacement. *Acta Crystallogr. A* **50**, 157–163 (1994).

24. Brunger, A. T. *et al.* Crystallography & NMR system: a new software suite for macromolecular structure determination. *Acta Crystallogr. D* **54**, 905–921 (1998).
25. Vagin, A. & Teplyakov, A. MOLREP: an automated program for molecular replacement. *J. Appl. Crystallogr.* **30**, 1022–1025 (1997).
26. Jones, T., Zou, J.-Y., Cowan, S. & Kjeldgaard, M. Improved methods for building protein models in electron density maps and the location of errors in these models. *Acta Crystallogr. A* **47**, 110–119 (1991).
27. Winn, M. D., Isupov, M. N. & Murshudov, G. N. Use of TLS parameters to model anisotropic displacements in macromolecular refinement. *Acta Crystallogr. D* **57**, 122–133 (2001).
28. Laskowski, R. A. *et al.* PROCHECK: a program to check the stereochemical quality of protein structures. *J. Appl. Crystallogr.* **26**, 283–291 (1993).
29. Carson, M. Ribbons. *Methods Enzymol.* **277**, 493–505 (1997).
30. Kraulis, P. J. A program to produce both detailed and schematic plots of protein structures. *J. Appl. Crystallogr.* **24**, 946–950 (1991).

Supplementary Information accompanies the paper on Nature's website (<http://www.nature.com/nature>).

Acknowledgements We thank C. Ogata and M. Becker for assistance at beamlines X4A and X25, respectively, of NSLS at Brookhaven National Laboratory; A. Ullrich for supplying a human HER2 complementary DNA; P. Longo for technical assistance; T. Garrett, S. Yokoyama and colleagues for supplying preprints in advance of publication; S. Yokoyama for coordinates of the EGF–EGFR complex; M. Lemmon, K. Ferguson, M. Amzel, J. Berg, S. Bouyain and W. Yang for discussion and comments on the manuscript; A. Guarne for help with figures; and N. Davidson for assistance with Herceptin. This work was supported by the NIH and the HHMI.

Competing interests statement The authors declare that they have no competing financial interests.

Correspondence and requests for materials should be addressed to D.J.L. (e-mail: dleahy@jhmi.edu). Coordinates and structure factors are available from the Protein Data Bank under accession numbers 1N8Y (rat sHER2) and 1N8Z (human sHER2–Herceptin Fab complex).

Crystal structure of the specificity domain of ribonuclease P

Andrey S. Krasilnikov*, Xiaojing Yang*, Tao Pan† & Alfonso Mondragón*

* Department of Biochemistry, Molecular Biology and Cell Biology, Northwestern University, Evanston, Illinois 60208, USA

† Department of Biochemistry and Molecular Biology, University of Chicago, 920 East 58th Street, Chicago, Illinois 60637, USA

RNase P is the only endonuclease responsible for processing the 5' end of transfer RNA by cleaving a precursor and leading to tRNA maturation^{1,2}. It contains an RNA component and a protein component and has been identified in all organisms. It was one of the first catalytic RNAs identified³ and the first that acts as a multiple-turnover enzyme *in vivo*. RNase P and the ribosome are so far the only two ribozymes known to be conserved in all kingdoms of life. The RNA component of bacterial RNase P can catalyse pre-tRNA cleavage in the absence of the RNase P protein *in vitro* and consists of two domains: a specificity domain and a catalytic domain^{4,5}. Here we report a 3.15-Å resolution crystal structure of the 154-nucleotide specificity domain of *Bacillus subtilis* RNase P. The structure reveals the architecture of this domain, the interactions that maintain the overall fold of the molecule, a large non-helical but well-structured module that is conserved in all RNase P RNA, and the regions that are involved in interactions with the substrate.

Bacterial RNase P can be subdivided into two major types (A and B) on the basis of their sequence characteristics. The best-characterized RNase P molecules come from two bacteria, *Escherichia coli* and *B. subtilis*, which are paradigms for the A- and B-type molecules, respectively. The RNA component of bacterial RNase P (P RNA) consists of 350–450 nucleotides, whereas the protein component (P protein) is a small, basic protein of about 120 amino acids. In *B. subtilis* P RNA, the specificity domain (S domain)

comprises nucleotides 86–239, and the catalytic domain (C domain) comprises the rest of the molecule (Fig. 1a). The S domain alone can bind pre-tRNA directly with micromolar affinity⁶.

The overall structure of the specificity domain is shown in Fig. 1b together with a diagram illustrating the secondary structure of the molecule (Fig. 1c). The S domain consists of several distinct secondary structure modules, which were predicted from the P RNA sequence and by phylogenetic comparison^{7,8}. Overall, the structure agrees very well with secondary structure predictions⁸, cross-linking data⁹ and Fe(II)-EDTA cleavage protection data¹⁰ (see Supplementary Information). The most salient features of the structure are (1) a junction formed by the stacked P7, P10 and P11 and the stacked P8 and P9 helices; (2) the packing of the P10.1 and P12 helices through a GAAA tetraloop–tetraloop receptor interaction; and (3) an unusually folded module linking P11 and P12 (J11/12–J12/11) (orange in Fig. 1), which contains a large number of universally conserved nucleotides, and is stabilized without canonical Watson–Crick base pairing. Although the S domain forms a well-packed and compact structure, it is important to note that the P11 and P9 helices together with the J11/12–J12/11 module form a clamp-like opening that contains nucleotides involved in pre-tRNA binding and is large enough to accommodate the TΨC stem-loop of a pre-tRNA molecule.

There are two molecules in the crystallographic asymmetric unit (1 and 2) related by a rotation of about 90°. It is unlikely that the crystallographic dimer observed is related to the dimer formed by the P RNA in the presence of the P protein in solution¹¹, as the intermolecular interactions observed in the crystal structure would lead to higher-order aggregates. The two molecules in the asymmetric unit are in slightly different conformations (see Supplementary Information). Molecule 1 has a disordered P12 helix and a partly disordered P10.1 helix (between bases A142 and G166). The tetraloop–tetraloop receptor interaction observed in molecule 2 is precluded in molecule 1 by crystal packing. Comparison of the two conformations suggests that the structure is built of relatively rigid structural elements and stabilized by a variety of interactions, such as stacking of helices, stacking of bulged bases, and the tetraloop–tetraloop receptor interaction. The central element of the S domain is a rigid core (red in Fig. 1), which has a practically identical conformation in both molecules in the asymmetric unit (root-mean-square deviation (r.m.s.d.) = 0.63 Å). The core is formed by the continuous stacking of stems P10 and P11, together with the basal portion of the P10.1 stem. The base of the P10.1 stem includes a loop spanning U175 to A179 (see Fig. 2a). The phylogenetically conserved U175 and A179 form a reversed Watson–Crick base pair that stabilizes the loop and serves as the starting base pair for the P10.1 helix, helping to align the P10.1 stem with respect to the core. Two conserved adenosines in the loop, A177 and A178, enter the minor groove of the P7/P10 stack in a region including conserved base pairs G90–C235 and G132–C234. This type of interaction, between conserved adenosines in a loop and conserved G–C base pairs in a helix, has recently been termed an A-minor motif¹². It includes contacts between the 2'-OH groups of the loop nucleotides with the 2'-OH groups of the helical residues similar to those in a ribose zipper¹³. The first four canonical Watson–Crick pairs in the P10.1 stem complete this portion of the rigid core. The second helix in the core is formed by the stacking of helices P10 and P11. This helix also stacks on stem P7 to form a large, continuous helix (Fig. 1). We do not include P7 in the rigid core because the P7/P10 stack is rather flexible (the angle between P7 and P10 differs by about 10° between molecules 1 and 2, as opposed to the P10/P11 stack in which the two molecules show identical conformations). The P11 stem includes bulged conserved adenosines A229 and A230 that do not form part of the helix.

The P7/P10/P11 helix is part of a large junction that also includes stacked helices P8 and P9. Figure 2b shows the topology of this complex junction. The general stacking of the helices is in agree-